Dyes and Pigments 96 (2013) 619–625

Contents lists available at SciVerse ScienceDirect

Dyes and Pigments

journal homepage: www.elsevier.com/locate/dyepig

Influence of the benzo[*d*]thiazole-derived π-bridges on the optical and photovoltaic performance of D–π–A dyes

Zhenhua Ci, Xiaoqiang Yu*, Ming Bao, Chaolei Wang, Tingli Ma*

State Key Laboratory of Fine Chemicals, Dalian University of Technology, Dalian 116023, China

ARTICLE INFO

Article history:
Received 17 September 2012
Received in revised form
30 October 2012
Accepted 2 November 2012
Available online 14 November 2012

Keywords:
Dye-sensitized solar cells
Organic dye
Triphenylamine
π-Conjugated bridge
Benzo[*d*]thiazole
Photon-to-current conversion efficiency

ABSTRACT

New metal-free organic sensitizers containing a benzo[*d*]thiazole or phenyl unit as the π-conjugated system, a triphenylamine as an electron donor, and a cyanoacrylic acid moiety as an electron acceptor were synthesized and used for dye-sensitized solar cells. Photophysical and electrochemical properties of these dyes were investigated, and their performances as sensitizers in solar cells were measured. The introduction of a benzo[*d*]thiazole unit into the molecular structure resulted in a high incident photon-to-current conversion efficiency (more than 70%) from 340 nm to 600 nm. One solar cell containing a benzo[*d*]thiazole unit, produced a η of 5.85% (J_{SC} = 10.63 mA cm^{-2}, V_{OC} = 0.72 V, and ff = 0.77) under 100 mW cm^{-2} simulated AM 1.5 G solar irradiation.

1. Introduction

Dye-sensitized solar cells (DSSCs) have attracted significant attention in recent years due to their high efficiency, low cost, and facile fabrication [1–3]. DSSCs based on Ru(II)-polypyridyl complex photosensitizers, such as N3, N719, and the black dye, have achieved remarkable conversion efficiency of up to 11% under AM 1.5 irradiation conditions [4–6]. However, the main drawbacks of the Ru(II) complex sensitizers include the cost of ruthenium metal, the requirement for cautious synthesis, and the tedious purification process. Metal-free organic dyes have gained increasing attention due to their unique advantages, such as high molar absorption coefficient, ease of structure modification, and relatively low material cost [7–10].

A common organic dye for DSSCs contains a structure of electron donor/acceptor (D–A) linked through a π-conjugated bridge, which is termed the D–π–A molecular structure [11]. Triphenylamine derivatives have been widely used as the electron donor (D), whereas a cyanoacrylic acid moiety acts as the electron acceptor (A) in this structure. D–π–A dyes based on triphenylamine moieties with various π-conjugated bridges, such as benzene [12–18], thiophene [19–22], thienothiophene [23–27], dithienothiophene [28,29], benzo[*b*]thiophene [30,31], or benzothiadiazole [32–35], have been designed and synthesized as efficient sensitizers to achieve high conversion efficiency in DSSC devices. The π-conjugated bridge has a great influence on photoelectronic properties of the D–π–A dyes. Thus, developing highly efficient D–π–A dyes with novel π-conjugated bridge applied in DSSCs is an area of strong current research activity.

This study presents three new organic dyes (**DBT1**, **DBT2**, and **DPB**) with a 2-methylbenzo[*d*]thiazole moiety or a phenyl group as π-conjugated bridge, a simple triphenylamine moiety as electron donor, and a cyanoacetic acid as electron acceptor, as shown in Fig. 1. The new sensitizers **DBT1** and **DBT2**, with a 2-methylbenzo[*d*]thiazole moiety as π-conjugated bridge have the following advantages: (i) the use of a 2-methylbenzo[*d*]thiazole unit can avoid the aggregation of the dye with its non-planar structure to achieve a high short-circuit current density, (ii) the introduction of electron-rich benzo[*d*]thiazole unit as π-conjugated bridge connecting with triphenylamine can extend the duration of the excited state.

2. Experimental section

2.1. General analytical measurements

All chemicals were used as received form commercial sources without purification. Solvents for chemical synthesis, such as

* Corresponding authors. Tel.: +86 411 84986181; fax: +86 411 84986180.
E-mail addresses: yuxiaoqiang@dlut.edu.cn (X. Yu), tinglima@dlut.edu.cn (T. Ma).

0143-7208/$ – see front matter © 2012 Elsevier Ltd. All rights reserved.
http://dx.doi.org/10.1016/j.dyepig.2012.11.004

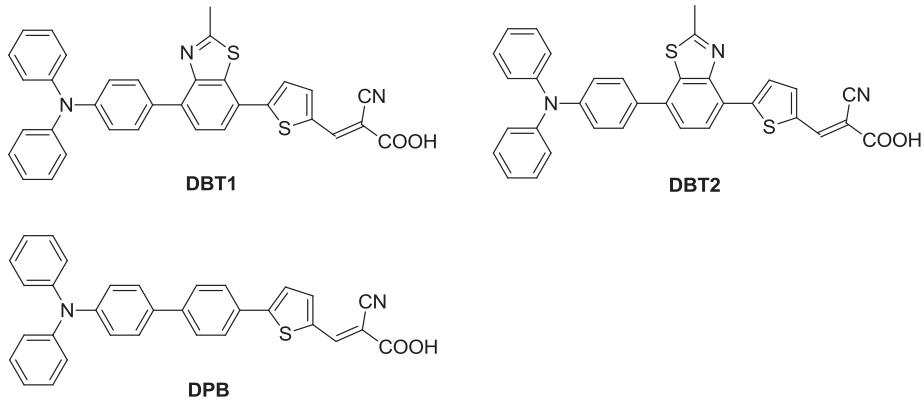

Fig. 1. Molecular structures of dyes **DBT1**, **DBT2**, and **DPB**.

dichloromethane, dimethylformamide, toluene, and tetrahydrofuran were purified by distillation. ^{1}H and ^{13}C NMR spectra were recorded on either Varian Inova-400 spectrometer (400 MHz for ^{1}H; 100 MHz for ^{13}C) or Bruker Avance II-400 spectrometer (400 MHz for ^{1}H; 100 MHz for ^{13}C); $CDCl_3$ and TMS were used as solvent and internal standard, respectively. High resolution mass spectra were recorded on either Q-TOF or GC-TOF mass spectrometer.

2.2. Theoretical calculations

Gaussian 03 package was used for density functional theory calculation [36]. The geometries and energies of **DBT1**, **DBT2**, and **DPB** were determined using the B3LYP method with the 6-31G (d) basis set.

2.3. Synthesis

The synthetic routes to **DBT1**, **DBT2**, and **DPB** dyes are shown in Scheme 1.

2.3.1. Synthesis of 2,5-dibromonitrobenzene (**2**) [37]

A mixture of nitric acid (90%, 4.6 g, 70 mmol) and concentrated sulfuric acid (75 mL) was added to a solution of 1,4-dibromobenzene (11.8 g, 50 mmol) in CH_2Cl_2 (30 mL) and concentrated sulfuric acid (20 mL) using a dropping funnel, and was allowed to react for 20 min at room temperature. The reaction mixture was stirred for 30 min, quenched with a solution of 25% aq. NaOH (3 mL), extracted with CH_2Cl_2 (30 mL), washed with water (10 mL), and dried over $MgSO_4$. Evaporation in vacuo afforded compound **2** (13.7 g, 97% yield) as light yellow crystals. mp 83–84 °C. ^{1}H NMR (400 MHz, $CDCl_3$) δ 7.98 (d, $J = 2.3$ Hz, 1H), 7.55–7.63 (m, 2H).

2.3.2. Synthesis of 2,5-dibromoacetanilide (**3**) [37]

A mixture of compound **2** (2.81 g, 10 mmol) and iron powder (5.5 g, 100 mmol) in AcOH (50 mL) was stirred for 5 h at 70 °C. The mixture was washed with water and extracted with ethyl acetate after cooling to room temperature. The organic layer was collected and dried over anhydrous $MgSO_4$. The solvent was removed under reduced pressure to afford 2,5-dibromoaniline (2.408 g, 96% yield). Acetyl chloride (0.83 g, 10.6 mmol) was slowly added to a solution of the foregoing 2,5-dibromoaniline (2.408 g, 9.6 mmol) in pyridine (20 mL), and the resulting mixture was heated under reflux for 1 h. The reaction mixture was poured into water (100 mL) after cooling to room temperature. The resulting precipitate was collected by vacuum filtration, and then recrystallized from methanol to obtain product **3** as white solid (2.27 g, 78% yield). mp 173–175 °C. ^{1}H NMR (400 MHz, $CDCl_3$) δ 8.59 (br s, 1H), 7.57 (br s, 1H), 7.38 (d, $J = 8.8$ Hz, 1H), 7.10 (dd, $J = 8.5$, 2.4 Hz, 1H), 2.25 (s, 3H).

2.3.3. Synthesis of N-(2,5-dibromophenyl)ethanethioamide (**4**) [38]

A solution of compound **3** (2.93 g, 10 mmol) and hexamethyldisiloxane (HMDO) (2.92 g, 18 mmol) in toluene (50 mL) was added to phosphorus pentasulfide (0.72 g, 3.25 mmol) at 60 °C, and the mixture was heated under reflux for 5 h. The crude product was purified by column chromatography (petroleum ether/ethyl acetate = 10/1, v/v) to obtain the desired product **4** as yellow–orange solid (2.66 g, 86% yield). mp 121–123 °C. ^{1}H NMR (400 MHz, $CDCl_3$) δ 8.77 (s, 1H), 7.48 (d, $J = 8.5$ Hz, 1H), 7.27 (d, $J = 8.6$ Hz, 1H), 2.78 (s, 3H).

2.3.4. Synthesis of 4,7-dibromo-2-methylbenzo[d]thiazole (**5**)

A mixture of compound **4** (3.09 g, 10 mmol) and sodium hydroxide (3.2 g, 80 mmol) in water–ethanol (40 mL–2 mL) was added dropwise to a solution of potassium ferricyanide (13.17 g, 40 mmol) in water (20 mL) and stirred at 95 °C for 2 h. The reaction mixture was cooled in an ice bath to yield the precipitate. Subsequently, the precipitate was filtered, washed with water, and concentrated in vacuo. The crude product was purified by column chromatography (petroleum ether/ethyl acetate = 20/1, v/v) to obtain the desired product **5** as pale yellow powder (1.46 g, 48% yield). mp 153–155 °C. IR (KBr): 3080, 2919, 1856, 1522, 1446, 1372, 1339, 1170, 1113, 1087, 909, 798. ^{1}H NMR (400 MHz, $CDCl_3$) δ 7.52 (d, $J = 8.4$ Hz, 1H), 7.34 (d, $J = 8.4$ Hz, 1H), 2.88 (s, 3H). ^{13}C NMR (100 MHz, $CDCl_3$) δ 168.7, 151.1, 139.2, 130.4, 128.4, 115.0, 112.9, 20.7. HRMS (EI, *m/z*): calcd. for $C_8H_5NSBr_2$, 304.8509 $[M]^+$; found, 304.8509.

2.3.5. Synthesis of 4-(7-bromo-2-methylbenzo[d]thiazol-4-yl)-N,N-diphenylaniline (**7a**) and 4-(4-bromo-2-methylbenzo[d]thiazol-7-yl)-N,N-diphenylaniline (**7b**) [39]

A mixture of compound **5** (0.307 g, 1 mmol), *N,N*-diphenyl-4-aminophenylboronic acid (0.289 g, 1 mmol), $Pd(PPh_3)_4$ (0.116 g, 0.1 mmol), and Na_2CO_3 (0.106 g, 1 mmol) was dissolved in toluene–THF–H_2O (1 mL–1 mL–0.2 mL) and was heated under reflux for 24 h under nitrogen atmosphere. Water was added to quench the reaction after the reaction was completed. The mixture was then extracted with diethyl ether, dried over anhydrous $MgSO_4$, and evaporated under vacuum. The crude product was purified by column chromatography (petroleum ether/ethyl acetate = 20/1, v/v) to afford two fractions. Fractions 1 product **7a** (0.132 g, 28% yield). mp 151–153 °C. IR (KBr): 3053, 3032, 1589, 1509, 1490, 1459, 1277, 1170, 909, 835, 816, 805, 755, 696, 656, 535, 509. ^{1}H NMR

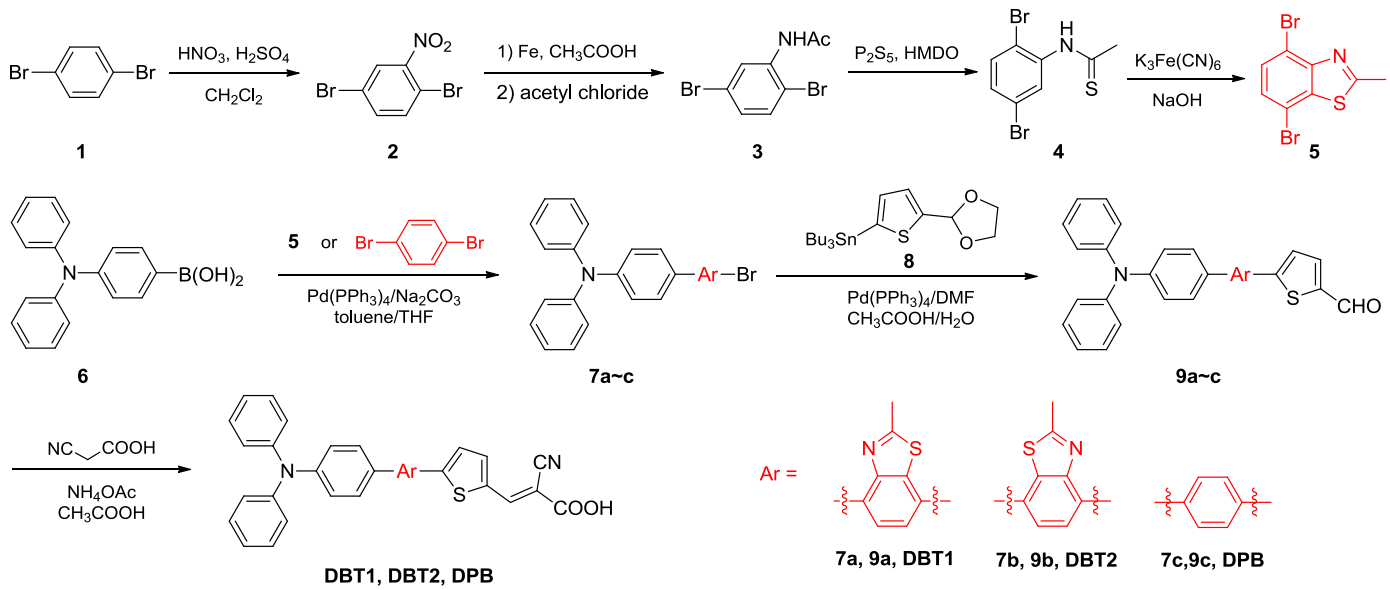

Scheme 1. Synthesis of the dyes (**DBT1**, **DBT2**, and **DPB**).

(400 MHz, d_6-DMSO) δ 7.76 (d, J = 8.6 Hz, 2H), 7.68 (d, J = 8.1 Hz, 1H), 7.53 (d, J = 8.1 Hz, 1H), 7.35 (dd, J = 7.8, 8.0 Hz, 4H), 7.10–7.05 (m, 8H), 2.83 (s, 3H). ^{13}C NMR (100 MHz, d_6-DMSO) δ 167.2, 150.0, 147.4, 139.1, 133.8, 131.8, 130.9, 130.1, 128.2, 127.7, 124.8, 123.8, 111.2, 20.6. HRMS (EI, m/z): calcd. for $C_{26}H_{19}N_2SBr$, 470.0452 [M]$^+$; found, 470.0446.

Fraction 2 product 7b (24% yield). mp 149–151 °C. IR (KBr): 3031, 2921, 1590, 1511, 1488, 1462, 1275, 1175, 921, 810, 751, 695, 643, 581, 539. ^{1}H NMR (400 MHz, d_6-DMSO) δ 7.80 (d, J = 8.0 Hz, 2H), 7.59 (d, J = 8.7 Hz, 2H), 7.41–7.34 (m, 5H), 7.14–7.06 (m, 8H), 2.83 (s, 3H). ^{13}C NMR (100 MHz, d_6-DMSO) δ 168.9, 151.6, 148.1, 147.2, 135.1, 135.0, 132.7, 130.3, 130.2, 128.9, 125.4, 125.1, 124.2, 122.7, 114.1, 20.2. HRMS (EI, m/z): calcd. for $C_{26}H_{19}N_2SBr$, 470.0452 [M]$^+$; found, 470.0457.

2.3.6. Synthesis of 4'-bromo-N,N-diphenyl-[1,1'-biphenyl]-4-amine (*7c*)

The synthetic route of **7c** is similar with **7a** to give orange solid in 64% yield. mp 180–181 °C. IR (KBr): 3446, 3064, 3035, 1589, 1481, 1337, 1277, 814, 748, 695. ^{1}H NMR (400 MHz, d_6-DMSO) δ 7.52 (d, J = 8.6 Hz, 2H), 7.42 (dd, J = 8.7, 1.3 Hz, 4H), 7.26 (dd, J = 6.8, 1.8 Hz, 4H), 7.12–7.04 (m, 8H). ^{13}C NMR (100 MHz, d_6-DMSO) δ 147.6, 147.4, 139.2, 133.0, 132.2, 130.1, 128.6, 1278.0, 124.7, 123.8, 123.5, 120.7. HRMS (EI, m/z): calcd. for $C_{24}H_{18}BrN$, 399.0623 [M]$^+$; found, 399.0617.

2.3.7. Synthesis of 5-(4-(4-(diphenylamino)phenyl)-2-methylbenzo[d]thiazol-7-yl)thiophene-2-carbaldehyde (*9a*)

A mixture of **7a** (0.471 g, 1 mmol), 2-tributylstannyl-5-dioxolanyl thiophene (0.49 g, 1.1 mmol), and $Pd(PPh_3)_4$ (0.116 g, 0.1 mmol) in dry DMF (10 mL) was heated at 80 °C for 18 h under nitrogen atmosphere. Water was added to quench the reaction when the reaction was completed. The resulting mixture was then extracted with diethyl ether, dried over anhydrous $MgSO_4$, and evaporated under vacuum to obtain the crude dioxolane derivative. The dioxolane derivative was suspended in glacial acetic acid (5 mL) and heated at 50 °C. Water (1 mL) was added after a clear solution was formed, and temperature was maintained at 50 °C for 5 h. The reaction was then cooled by adding ice water (10 mL) into the mixture. Afterward, the resulting orange precipitate was filtered with water and washed with methanol. The residue was purified by column chromatography on silica (petroleum ether/ethyl acetate = 5/1, v/v) to obtain product **9a** as yellow solid (0.452 g, 90%). mp 156–157 °C. IR (KBr): 3433, 3032, 2922, 1894, 1659, 1588, 1511, 1488, 1276, 877, 807, 753. ^{1}H NMR (400 MHz, d_6-DMSO) δ 9.99 (s, 1H), 8.17 (d, J = 4.0 Hz, 1H), 7.94 (d, J = 8.0 Hz, 1H), 7.89 (d, J = 4.0 Hz, 1H), 7.84 (m, 2.0 Hz, 2H), 7.72 (d, J = 8.0 Hz, 1H), 7.36 (t, J = 8.0 Hz, 4H), 7.12–7.06 (m, 8H), 2.87 (s, 3H). ^{13}C NMR (100 MHz, d_6-DMSO) δ 184.7, 167.3, 151.4, 150.9, 147.6, 147.4, 142.9, 139.2, 135.5, 134.6, 1312.0, 131.1, 130.1, 127.4, 126.9, 126.0, 125.2, 125.0, 123.9, 122.6, 20.4. HRMS (EI, m/z): calcd. for $C_{31}H_{22}N_2OS_2$, 502.1174 [M]$^+$; found, 502.1175.

2.3.8. Synthesis of 5-(7-(4-(diphenylamino)phenyl)-2-methylbenzo[d]thiazol-4-yl)thiophene-2-carbaldehyde (*9b*)

The synthetic route of **9b** is similar with **9a** to give yellow solid in 82% yield. mp 154–156 °C. IR (KBr): 3430, 3034, 2922, 1662, 1589, 1512, 1487, 1273, 804, 697. ^{1}H NMR (400 MHz, d_6-DMSO) δ 9.97 (s, 1H), 8.18 (d, J = 4.0 Hz, 1H), 8.16 (d, J = 7.4 Hz, 1H), 8.08 (d, J = 4.1 Hz, 1H), 7.66 (d, J = 8.7 Hz, 2H), 7.59 (d, J = 8.0 Hz, 1H), 7.37 (dd, J = 7.8, 8.1 Hz, 4H), 7.15–7.07 (m, 8H), 2.92 (s, 3H). ^{13}C NMR (100 MHz, d_6-DMSO) δ 184.9, 168.9, 149.8, 149.1, 148.2, 147.2, 143.9, 138.2, 135.3, 132.8, 130.2, 129.1, 127.6, 125.7, 125.2, 124.9, 124.6, 124.3, 122.6, 20.5. HRMS (EI, m/z): calcd. for $C_{31}H_{22}N_2OS_2$, 502.1174 [M]$^+$; found, 502.1175.

2.3.9. Synthesis of 5-(4'-(diphenylamino)-[1,1'-biphenyl]-4-yl) thiophene-2-carbaldehyde (*9c*)

The synthetic route of **9c** is similar with **9a** to give yellow solid in 71% yield. mp 180–182 °C. IR (KBr): 3443, 3031, 2957, 2924, 2794, 1666, 1591, 1519, 1491, 1450, 1326, 1274, 818, 800, 751. ^{1}H NMR (400 MHz, d_6-DMSO) δ 9.92 (s, 1H), 8.06 (d, J = 3.7 Hz, 1H), 7.86 (d, J = 8.1 Hz, 2H), 7.79 (d, J = 3.6 Hz, 1H), 7.74 (d, J = 8.2 Hz, 2H), 7.66 (d, J = 8.4 Hz, 2H), 7.33 (dd, J = 7.8, 7.5 Hz, 4H), 7.11–7.03 (m, 8H). ^{13}C NMR (100 MHz, d_6-DMSO) δ 184.4, 152.8, 147.7, 147.4, 142.3, 141.0, 139.7, 133.0, 131.4, 130.1, 128.0, 127.3, 127.2, 125.6, 124.8, 123.9, 123.4. HRMS (EI, m/z): calcd. for $C_{29}H_{21}NOS$, 431.1344 [M]$^+$; found, 431.1337.

2.3.10. Synthesis of 2-cyano-3-(5-(4-(4-(diphenylamino)phenyl)-2-methylbenzo[d]thiazol-7-yl)thiophen-2-yl) acrylic acid (*DBT1*)

A mixture of **9a** (1 mmol, 0.503 g), cyanoacetic acid (1.1 mmol, 0.094 g), ammonium acetate (0.25 mmol, 0.02 g), and acetic acid (5 mL) was heated to reflux for 5 h under nitrogen atmosphere. The

mixture was subsequently cooled to room temperature, poured into ice water, and extracted with ethyl acetate. The organic layer was collected, dried over anhydrous $MgSO_4$, and evaporated under vacuum. The crude product was purified by column chromatography on silica (DCM/ethanol = 20/1, v/v) to obtain **DBT1** as a red solid (0.453 g, 76%). mp 238–240 °C. IR (KBr): 3447, 2211, 1636, 1591, 1508, 1490, 1438, 1358, 1279, 1177, 753, 697. ^{1}H NMR (400 MHz, d_6-DMSO) δ 8.59 (s, 1 H), 8.13 (d, J = 4.0 Hz, 1H), 7.94 (d, J = 8.0 Hz, 1H), 7.90 (d, J = 4.0 Hz, 1H), 7.84 (d, J = 8.0 Hz, 2H), 7.72 (d, J = 8.0 Hz, 1H), 7.35 (t, J = 8.0 Hz, 4H), 7.12–7.06 (m, 8H), 2.88 (s, 3H). ^{13}C NMR (100 MHz, d_6-DMSO) δ 167.2, 151.4, 147.5, 147.4, 139.7, 132.1, 131.1, 130.1, 126.9, 126.2, 125.4, 124.9, 123.9, 122.7, 30.9. HRMS (ES, m/z): calcd. for $C_{34}H_{22}N_3O_2S_2$, 568.1153 $[M]^+$; found, 568.1161.

2.3.11. Synthesis of 2-cyano-3-(5-(7-(4-(diphenylamino)phenyl)-2-methylbenzo[d]thiazol-4-yl)thiophen-2-yl) acrylic acid (*DBT2*)

The synthetic route of **DBT2** is similar with **DBT1** to give red solid in 71% yield. mp 240–242 °C. IR (KBr): 3448, 2214, 1613, 1593, 1517, 1490, 1433, 1384, 1332, 1282, 1220, 1177, 809, 752, 697. ^{1}H NMR (400 MHz, d_6-DMSO) δ 8.52 (s, 1H), 8.21 (d, J = 4.2 Hz, 1H), 8.14 (d, J = 8.1 Hz, 1H), 8.07 (d, J = 4.3 Hz, 1H), 7.66 (d, J = 8.7 Hz, 2H), 7.60 (d, J = 8.0 Hz, 1H), 7.37 (dd, J = 8.0, 7.9 Hz, 4H), 7.15–7.07 (m, 8H), 2.89 (s, 3H). ^{13}C NMR (100 MHz, d_6-DMSO) δ 168.7, 149.6, 148.2, 147.2, 135.4, 132.2, 132.0, 130.2, 129.1, 129.1, 127.8, 125.6, 125.2, 125.1, 124.3, 122.7, 29.5. HRMS (ES, m/z): calcd. for $C_{34}H_{22}N_3O_2S_2$, 568.1153 $[M]^+$; found, 568.1160.

2.3.12. Synthesis of 2-cyano-3-(5-(4'-(diphenylamino)-[1,1'-biphenyl]-4-yl)thiophen-2-yl) acrylic acid (*DPB*)

The synthetic route of **DPB** is similar with **DBT1** to give red solid in 81% yield. mp 248–249 °C. IR (KBr): 3431, 3031, 2974, 2219, 1684, 1583, 1488, 1422, 1365, 1327, 1282, 1224, 821, 802, 750, 696. ^{1}H NMR (400 MHz, d_6-DMSO) δ 8.43 (s, 1H), 7.97 (d, J = 4.0 Hz, 1H), 7.83 (d, J = 8.3 Hz, 2H), 7.78 (d, J = 4.1 Hz, 1H), 7.75 (d, J = 8.4 Hz, 2H), 7.65 (d, J = 8.6 Hz, 2H), 7.33 (dd, J = 7.8, 7.8 Hz, 4H), 7.11–7.03 (m, 8H). ^{13}C NMR (100 MHz, d_6-DMSO) δ 164.2, 151.8, 147.7, 147.4, 145.6, 140.8, 140.7, 135.3, 133.0, 131.3, 130.1, 128.0, 127.3, 127.1, 125.4, 124.8, 123.9, 123.4, 117.7. HRMS (EI, m/z): calcd. for $C_{32}H_{22}N_2O_2S$, 498.1402 $[M]^+$; found, 498.1404.

2.4. Fabrication of DSSCs

The screen-printable TiO_2 pastes were prepared according to the procedure developed by Ma's group [40]. A screen-printing technique was used to fabricate TiO_2 films. First, The paste was deposited on a fluorine-doped tin oxide conductive glass (FTO, Asahi Glass Co., Ltd.; sheet resistance: 10 ohm/sq). Second, the film was sintered at 450 °C for 30 min in atmospheric air, and then immersed in 40 mM $TiCl_4$ solution for 30 min at 70 °C, rinsed with water and ethanol, and sintered at 500 °C for 30 min. The film was dipped into **DBT1**, **DBT2**, and **DPB** dye solutions (0.4 mM in THF) for 18 h after cooling to 80 °C. Finally, dye-sensitized TiO_2 photoelectrodes (thickness: 12 μm) were obtained. The organic electrolyte was composed of 0.06 M LiI, 0.03 M I_2, 0.1 M guanidinium thiocyanate, 0.6 M 1-propyl-3-methylimidazolium iodide (PMII), and 0.5 M *tert*-butyl-pyridine in acetonitrile. The active area of DSSCs was 0.16 cm^2. DSSC devices were assembled with counter electrodes (thermally platinized FTO) using a thermoplastic frame (Surlyn, 60 μm thick).

2.5. Measurements

Absorption and emission spectra were recorded with HP8453 (USA) and PTI700 (USA), respectively. Electrochemical measurement was carried out on a BAS100W (USA) electrochemistry workstation. The irradiation source for the photocurrent–voltage (J–V) measurement was an AM 1.5 solar simulator (16S-002, Solar Light Co. Ltd., USA). The incident light intensity was 100 mW cm^{-2} calibrated with a standard silicon solar cell. The current–voltage curve was obtained by linear sweep voltammetry (LSV) method using an electrochemical workstation (LK9805, Lanlike Co. Ltd., China). The incident photon-to-current conversion efficiency (IPCE) measurement was performed by a Hypermonolight (SM-25, Jasco Co. Ltd., Japan).

3. Results and discussion

3.1. Synthesis

DBT1, **DBT2**, and **DPB** dyes were synthesized using the stepwise synthetic procedure (Scheme 1). The nitration reaction of 1,4-dibromobenzene (**1**) produced 2,5-dibromonitrobenzene (**2**). The reduction of the nitro group was realized following a standard protocol using iron powder in acetic acid to afford 2,5-dibromoaniline. Benzanilide (**3**) was prepared from 2,5-dibromoaniline by reaction with acetylchloride, which was then efficiently transformed into thiobenzanilide (**4**) by reaction with Lawesson's reagent. Regiospecific cyclization of **4** using potassium ferricyanide and aqueous sodium hydroxide produced 4,7-dibromo-2-methylbenzo[*d*]thiazole (**5**). The Suzuki cross-coupling reaction of **5** or **1** with arylboronic acid **6** afforded the corresponding products **7a**–**7c** [41]. The Stille cross-coupling reaction of **7a**–**7c** with organotin compound **8**, followed with deprotection reaction to afford the free aldehydes **9a**–**9c**. Finally, the aldehydes were condensed with cyanoacetic acid to obtain the target compounds **DBT1**, **DBT2**, and **DPB** via Knöevenagel reaction, in the presence of ammonium acetate [42].

3.2. Absorption properties in solutions

The optical and electrochemical properties of the three dyes are summarized in Fig. 2 and Table 1. Fig. 2 shows that all dyes in THF solutions gave two distinct absorption bands: one relatively weak band in the near-UV region (300 nm–310 nm) that corresponds to the π–π^* electron transition and the other one has a strong absorption in the visible region (420 nm–460 nm), which can be assigned to an intramolecular charge transfer (ICT) between the triarylamine donating unit and the cyanoacrylic acid anchoring moiety, thereby producing an efficient charge-separated state. Compared with **DPB**, the maximum absorptions of **DBT1** and **DBT2**

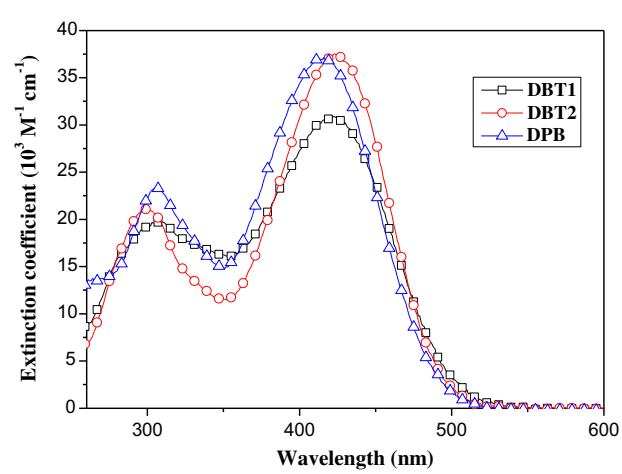

Fig. 2. Absorption spectra of **DBT1**, **DBT2**, and **DPB** in THF at ambient temperature.

Table 1
Optical and electrochemical properties of **DBT1**, **DBT2**, and **DPB** dyes.

Dye	Absorption[a]		Emission[a]	Oxidation potential		
	λ_{max} [nm]	ε at λ_{max} [M^{-1} cm^{-1}]	λ_{max} [nm]	E_{ox} [V][b] (versus NHE)	E_{0-0} [V][c] (Abs/Em)	E_{LUMO} [V] (versus NHE)
DBT1	420	30,902	592	1.13	2.51	−1.38
DBT2	423	37,531	573	1.16	2.55	−1.39
DPB	416	37,148	583	1.12	2.62	−1.50

[a] Absorption and emission spectra were measured in THF, with a concentration of 1.0×10^{-3} M at room temperature.
[b] The oxidation potential of the dyes was measured under the following conditions: working electrode, Pt; electrolyte, 0.1 M tetrabutylammonium hexafluorophosphate, n-Bu_4NPF_6 in THF; scan rate, 0.1 V/s. Potentials measured vs Fe^+/Fe were converted to NHE by addition of +0.63 V [44].
[c] The E_{0-0} energies were estimated from the intercept of the normalized absorption and emission spectra.

were slightly distant due to the expansion of the π-conjugation system due to the introduction of the benzo[*d*]thiazole unit into the π-conjugated bridge. Noticeably, the molar extinction coefficients of the three dyes were higher than that of the N719 dye ($14.0\ M^{-1}\ cm^{-1} \times 10^3\ M^{-1}\ cm^{-1}$) [5], indicating a good light harvesting ability.

3.3. Molecular orbital calculations

The molecular geometries and electron distributions of **DBT1**, **DBT2**, and **DPB** were obtained using the density function theory (DFT) calculations with Gaussian 03 program. The calculations were performed with the B3LYP exchange correlation functional under 6-31G (d) basis. The results are shown in Fig. 3. The electron distribution before the light irradiation locates mainly on the donor units; whereas it moves to the acceptor units close to the anchoring groups after light irradiation, which favors the electron injection from the dye molecules to the conduction band edge of TiO_2.

3.4. Electrochemical properties

The redox behavior of **DBT1**, **DBT2**, and **DPB** dyes were studied by cyclic voltammetry (in Fig. 4) to investigate the ability of electron transfer from the excited dye molecules to the conductive band of TiO_2. The cyclic voltammograms of these dyes were measured in a solution of 0.1 M n-Bu_4NPF_6 in THF. A three-electrode cell containing a Pt-coil working electrode, a Pt wire counter electrode, and a Ag/AgCl reference electrode was employed. The ferrocene/ferricenium (Fc/Fc^+) redox couple was used as an internal reference. The examined highest occupied molecular orbital (HOMO) levels and the lowest unoccupied molecular orbital (LUMO) levels were collected, as shown in Table 1. HOMO values of (1.12 V–1.16 V vs. NHE) were more positive than the I^-/I_3^- redox couple (0.4 V vs. NHE), suggesting that the oxidized dyes can thermodynamically accept electrons from I^- ion in iodide/triiodide electrolyte for regeneration. Electron injection from the excited sensitizers to the conduction band of TiO_2 should be energetically favorable because of the more negative LUMO values (−1.38 V to −1.50 V vs. NHE) compared with the conduction band edge energy level of the TiO_2 electrode (at approximately −0.5 V vs NHE) [43]. These results clearly demonstrate that the novel dyes are potentially efficient dyes for DSSCs. Table 1 also shows that the introduction of the benzo[*d*]thiazole bridge can change the HOMO–LUMO energy gaps of the dyes more narrowly.

3.5. Photovoltaic performance

The action spectrum, the incident photon-to-electron conversion efficiency (IPCE) as a function of wavelength, was measured to evaluate the photoresponse of the photoelectrode in the whole spectral region. **DBT1**, **DBT2**, and **DPB** sensitizers were used to manufacture solar cell devices. Fig. 5 shows the IPCE obtained with 0.06 M LiI, 0.03 M I_2, 0.1 M guanidinium thiocyanate, 0.6 M 1-propyl-3-methylimidazolium iodide (PMII), and 0.5 M *tert*-butyl-

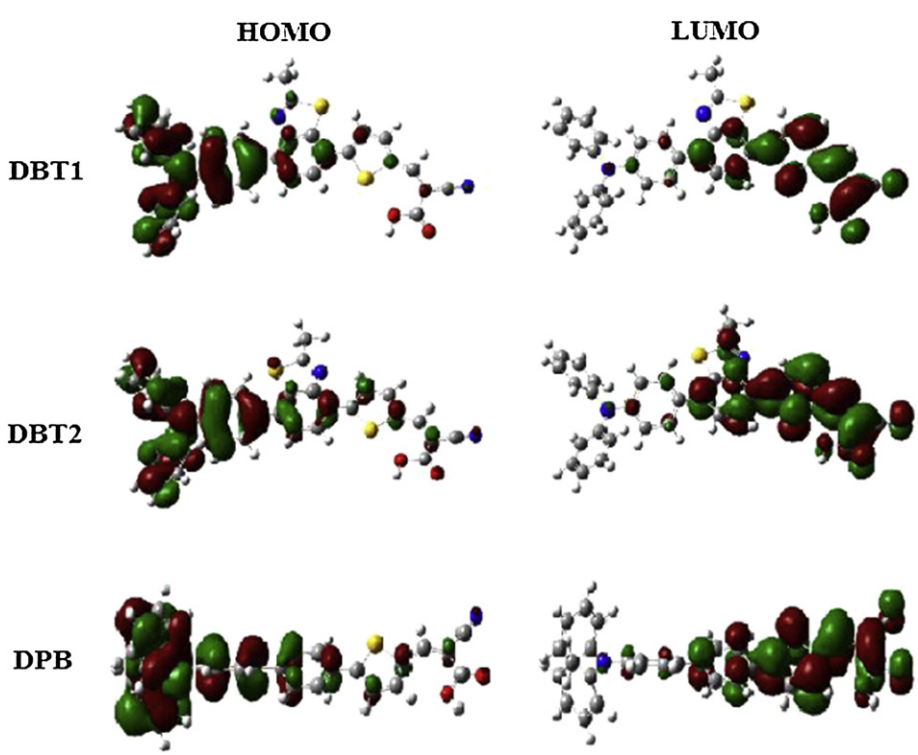

Fig. 3. Frontier HOMO and LUMO orbitals of **DBT1**, **DBT2**, and **DPB** dyes.

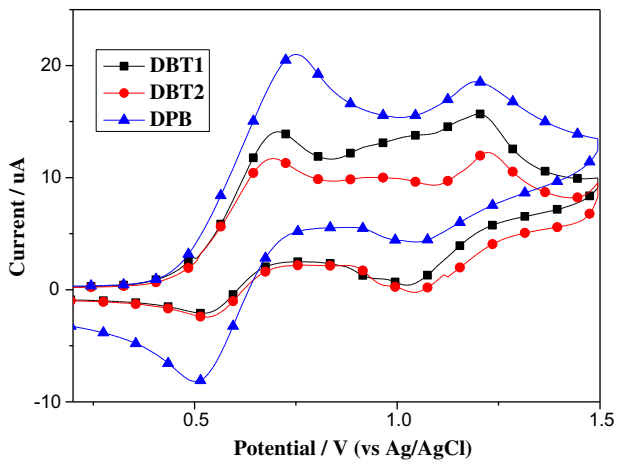

Fig. 4. Cyclic voltammogram of **DBT1**, **DBT2**, and **DPB** in THF.

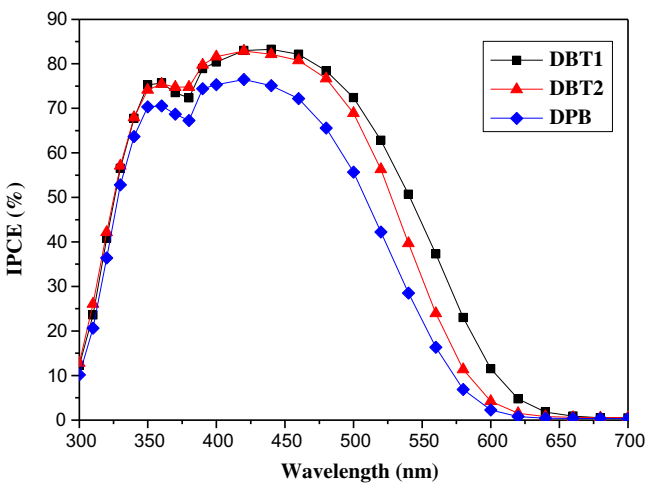

Fig. 5. IPCE spectra for DSSCs based on the as-synthesized dyes.

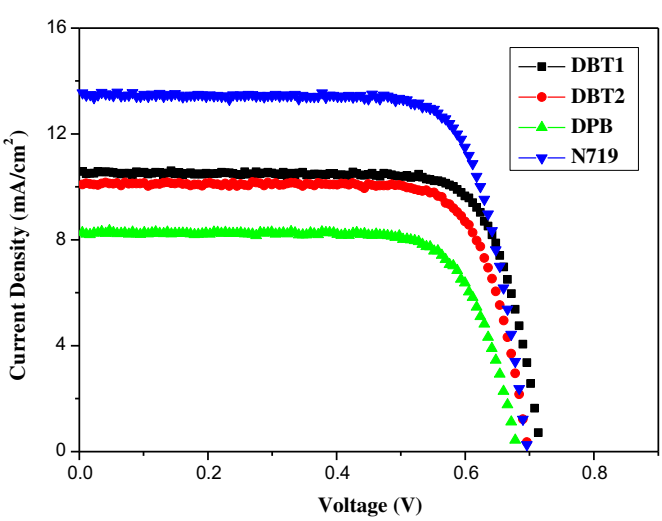

Fig. 6. Current–potential (J–V) curve for the DSSCs based on **DBT1**, **DBT2**, **DPB**, and **N719**.

Table 2
Photovoltaic performance of DSSCs sensitized with the as-synthesized dyes compared with the N719 dye.[a]

Dye	CDCA	J_{SC}/mA cm^{-2}	V_{OC}/mV	ff	η/%
DBT1	0 mM	10.63	0.72	0.77	5.85
	0.8 mM	11.01	0.71	0.78	6.08
DBT2	0 mM	10.04	0.70	0.77	5.43
	0.8 mM	10.43	0.71	0.76	5.63
DPB	0 mM	8.38	0.68	0.76	4.24
	0.8 mM	9.44	0.68	0.75	4.82
N719	0 mM	13.54	0.70	0.76	7.16

[a] The DSSCs had an active area of ~0.16 cm^2 and used an electrolyte composed of 0.06 M LiI, 0.03 M I_2, 0.1 M guanidinium thiocyanate, 0.6 M 1-propyl-3-methylimidazolium iodide (PMII), and 0.5 M *tert*-butyl-pyridine in acetonitrile.

pyridine in acetonitrile as redox electrolyte. The three dyes can efficiently convert visible-light to photocurrent in the region of 300 nm–600 nm. A solar cell based on **DBT1** showed the highest IPCE value of 83% at 440 nm. In addition the cell exhibited a broad IPCE spectrum with high IPCE values (>70%) from 340 nm to 500 nm. The IPCE spectrum of the DSSCs based on **DBT2** was similar to that based on **DBT1**. However, the IPCE spectrum of **DPB** was slightly lower, with a maximum IPCE of 76% at 420 nm.

Fig. 6 shows the current–voltage (J–V) curves of the DSSCs based on dyes **DBT1**, **DBT2**, and **DPB** under standard global AM 1.5 G solar irradiation, and the results are shown in Table 2. The DSSCs based on dye **DBT1** showed the best performance, with an open-circuit voltage of 0.72 V, a short-circuit photocurrent density of 10.63 mA cm^{-2}, and a fill factor of 0.77, yielding an overall conversion efficiency (η) of 5.85%. For a fair comparison, the N719-sensitized TiO_2 solar cell showed an efficiency of 7.16%, with a J_{SC} of 13.54 mA cm^{-2}, a V_{OC} of 0.70 V and a fill factor of 0.76. The conversion efficiency of **DBT1** ($\eta = 5.85\%$) reached 80% of the N719 cell efficiency ($\eta = 7.16\%$). Compared with the **DPB** based cells, the **DBT1** and **DBT2** based cells showed higher J_{SC} values, reflecting their better sunlight-harvesting ability due to the benzo[*d*]thiazole structure as a π-spacer.

Chenodeoxycholic acid (CDCA) is used as coadsorbent to dissociate the π-stacked dye aggregates and improve the electron-injection yield, thus affording higher J_{SC} value. For the DSSCs sensitized by the three dyes, the J_{SC} value of dye **DPB** with CDCA greatly increased (1.06 mA cm^{-2}) than that of **DBT1** and **DBT2** (<0.4 mA cm^{-2}) as shown in Table 2. The results indicate that the use of a 2-methylbenzo[*d*]thiazole unit can avoid the aggregation of the dyes with its non-planar structure to achieve a high short-circuit current density.

4. Conclusion

In summary, three new organic sensitizers (**DBT1**, **DBT2**, and **DPB**) containing benzo[*d*]thiazole or benzene structures as a π-conjugated spacer were designed and synthesized for dye-sensitized solar cells. The introduction of benzo[*d*]thiazole unit to tune the HOMO–LUMO levels increased the short circuit photocurrents (J_{SC}) and resulted in higher efficiencies. The cells based on **DBT1** and **DBT2**, with benzo[*d*]thiazole structures as π-conjugated spacers exhibited 5.85% and 5.43% conversion efficiencies, respectively, which are higher than that of **DPB** with the benzene moiety. Our results indicate that the benzo[*d*]thiazole moiety can be advantageously incorporated into the dye-sensitizer as a π-spacer to improve cell conversion efficiency. Further improvement of the power conversion efficiency of D–π–A dyes can be investigated by using benzo[*d*]thiazole as a π-conjugated spacer based on different donors.

Acknowledgments

We are grateful to the National Natural Science Foundation of China (No. 21002010 and 20923006) for their financial support. This work was also supported by the Fundamental Research Funds for the Central Universities (DUT12LK44 and DUT10RC(3)28).

References

[1] O'Regan B, Grätzel M. A low-cost, high-efficiency solar cell based on dye-sensitized colloidal TiO_2 films. Nature 1991;353:737–9.
[2] Grätzel M. Dye-sensitized solar cells. J Photochem Photobiol C 2003;4: 145–53.
[3] Grätzel M. Conversion of sunlight to electric power by nanocrystalline dye-sensitized solar cells. J Photochem Photobiol A 2004;164:3–14.
[4] Nazeeruddin MK, Kay A, Rodicio I, Humphry-Baker R, Müller E, Liska P, et al. Conversion of light to electricity by *cis*-X_2bis(2,2'-bipyridyl-4,4'-dicarboxylate) ruthenium(II) charge-transfer sensitizers ($X = Cl^-$, Br^-, I^-, CN^- and SCN^-) on nanocrystalline TiO_2 electrodes. J Am Chem Soc 1993;115:6382–90.
[5] Nazeeruddin MK, Zakeeruddin SM, Humphry-Baker R, Jirousek M, Liska P, Vlachopoulos N, et al. Acid–base equilibria of (2,2'-bipyridyl-4,4'-dicarboxylic acid) ruthenium(II) complexes and the effect of protonation on charge-transfer sensitization of nanocrystalline titania. Inorg Chem 1999; 38:6298–305.
[6] Nazeeruddin MK, Péchy P, Renouard T, Zakeeruddin SM, Humphry-Baker R, Comte P, et al. Engineering of efficient panchromatic sensitizers for nanocrystalline TiO_2-based solar cells. J Am Chem Soc 2001;123:1613–24.
[7] Ning ZJ, Zhang Q, Wu WJ, Pei HC, Liu B, Tian H. Starburst triarylamine based dyes for efficient dye-sensitized solar cells. J Org Chem 2008;73:3791–7.
[8] Wiberg J, Marinado T, Hagberg DP, Sun LC, Hagfeldt A, Albinsson B. Distance and driving force dependencies of electron injection and recombination dynamics in organic dye-sensitized solar cells. J Phys Chem B 2010;114: 14358–63.
[9] Chang DW, Lee HJ, Kim JH, Park SY, Park SM, Dai LM, et al. Novel quinoxaline-based organic sensitizers for dye-sensitized solar cells. Org Lett 2011;13: 3880–3.
[10] Gao FF, Wang Y, Shi D, Zhang J, Wang MK, Jing XY, et al. Enhance the optical absorptivity of nanocrystalline TiO_2 film with high molar extinction coefficient ruthenium sensitizers for high performance dye-sensitized solar cells. J Am Chem Soc 2008;130:10720–8.
[11] Späth M, Sommeling PM, van Roosmalen JAM, Smit HJP, van der Burg NPG, Mahieu DR, et al. Reproducible manufacturing of dye-sensitized solar cells on a semi-automated baseline. Prog Photovolt 2003;11:207–20.
[12] Hwang S, Lee JH, Park C, Lee H, Kim C, Park C, et al. A highly efficient organic sensitizer for dye-sensitized solar cells. Chem Commun 2007:4887–9.
[13] Kitamura T, Ikeda M, Shigaki K, Inoue T, Anderson NA, Ai X, et al. Phenyl-conjugated oligoene sensitizers for TiO_2 solar cells. Chem Mater 2004;16: 1806–12.
[14] Chen KF, Hsu YC, Wu QY, Yeh MCP, Sun SS. Structurally simple dipolar organic dyes featuring 1,3-cyclohexadiene conjugated unit for dye-sensitized solar cells. Org Lett 2009;11:377–80.
[15] Yang CH, Chen HL, Chuang YY, Wu CG, Chen CP, Liao SH, et al. Characteristics of triphenylamine-based dyes with multiple acceptors in application of dye-sensitized solar cells. J Power Sources 2009;188:627–34.
[16] Liang M, Xu W, Cai FS, Chen PQ, Peng B, Chen J, et al. New triphenylamine-based organic dyes for efficient dye-sensitized solar cells. J Phys Chem C 2007;111:4465–72.
[17] Kim C, Choi H, Kim S, Baik C, Song K, Kang MS, et al. Molecular engineering of organic sensitizers containing *p*-phenylene vinylene unit for dye-sensitized solar cells. J Org Chem 2008;73:7072–9.
[18] Xu W, Peng B, Chen J, Liang M, Cai FS. New triphenylamine-based dyes for dye-sensitized solar cells. J Phys Chem C 2008;112:874–80.
[19] Liu WH, Wu IC, Lai CH, Lai CH, Chou PT, Li YT, et al. Simple organic molecules bearing a 3,4-ethylenedioxythiophene linker for efficient dye-sensitized solar cells. Chem Commun 2008:5152–4.
[20] Hagberg DP, Marinado T, Karlsson KM, Nonomura K, Qin P, Boschloo G, et al. Tuning the HOMO and LUMO energy levels of organic chromophores for dye sensitized solar cells. J Org Chem 2007;72:9550–6.
[21] Shi D, Cao YM, Pootrakulchote N, Yi ZH, Xu MF, Zakeeruddin SM, et al. New organic sensitizer for stable dye-sensitized solar cells with solvent-free ionic liquid electrolytes. J Phys Chem C 2008;112:17478–85.
[22] Yum JH, Hagberg DP, Moon SJ, Karlsson KM, Marinado T, Sun LC, et al. A light-resistant organic sensitizer for solar-cell applications. Angew Chem Int Ed 2009;48:1576–80.
[23] Li G, Jiang KJ, Li YF, Li SL, Yang LM. Efficient structural modification of triphenylamine-based organic dyes for dye-sensitized solar cells. J Phys Chem C 2008;112:11591–9.
[24] Xu MF, Li RZ, Pootrakulchote N, Shi D, Guo J, Yi ZH, et al. Energy-level and molecular engineering of organic D-π-A sensitizers in dye-sensitized solar cells. J Phys Chem C 2008;112:19770–6.
[25] Wang MK, Xu MF, Shi D, Li RZ, Gao FF, Zhang GL, et al. High-performance liquid and solid dye-sensitized solar cells based on a novel metal-free organic sensitizer. Adv Mater 2008;20:4460–3.
[26] Zhang GL, Bai Y, Li RZ, Shi D, Wenger S, Zakeeruddin SM, et al. Employ a bisthienothiophene linker to construct an organic chromophore for efficient and stable dye-sensitized solar cells. Energy Environ Sci 2009;2:92–5.
[27] Zhang GL, Bala H, Cheng YM, Shi D, Lv XJ, Yu QJ, et al. High efficiency and stable dye-sensitized solar cells with an organic chromophore featuring a binary π-conjugated spacer. Chem Commun 2009;2:198–200.
[28] Qin H, Wenger S, Xu M, Gao F, Jing X, Wang P, et al. An organic sensitizer with a fused dithienothiophene unit for efficient and stable dye-sensitized solar cells. J Am Chem Soc 2008;130:9202–3.
[29] Tian HN, Yang XC, Chen RK, Zhang R, Hagfeldt A, Sun LC. Effect of different dye baths and dye-structures on the performance of dye-sensitized solar cells based on triphenylamine dyes. J Phys Chem C 2008;112:11023–33.
[30] Choi H, Lee JK, Song K, Kang SO, Ko J. Novel organic dyes containing bis-dimethylfluorenyl amino benzo[*b*]thiophene for highly efficient dye-sensitized solar cell. Tetrahedron 2007;63:3115–21.
[31] Choi H, Baik C, Kang SO, Ko J, Kang MS, Nazeeruddin MK, et al. Highly efficient and thermally stable organic sensitizers for solvent-free dye-sensitized solar cells. Angew Chem Int Ed 2008;47:327–30.
[32] Velusamy M, Thomas KRJ, Lin JT, Hsu YC, Ho KC. Organic dyes incorporating low-band-gap chromophores for dye-sensitized solar cells. Org Lett 2005;7: 1899–902.
[33] Lee DH, Lee MJ, Song HM, Song BJ, Seo KD, Pastore M, et al. Organic dyes incorporating low-band-gap chromophores based on π-extended benzothiadiazole for dye-sensitized solar cells. Dyes Pigm 2011;91:192–8.
[34] Seo KD, Choi IT, Park YG, Kang S, Lee JY, Kim HK. Novel D–A–π–A coumarin dyes containing low band-gap chromophores for dye-sensitised solar cells. Dyes Pigm 2012;94:469–74.
[35] Haid S, Marszalek M, Mishra A, Wielopolski M, Teuscher J, Moser J, et al. Significant improvement of dye-sensitized solar cell performance by small structural modification in π-conjugated donor–acceptor dyes. Adv Funct Mater 2012;22:1291–302.
[36] Frisch MJ, Trucks GW, Schlegel HB, Scuseria GE, Robb MA, Cheeseman JR, et al. Gaussian 03, revision C.02. Wallingford, CT: Gaussian Inc.; 2004.
[37] Maya F, Tour JM. Synthesis of terphenyl oligomers as molecular electronic device candidates. Tetrahedron 2004;60:81–92.
[38] Mylari BL, Larson ER, Beyer TA, Zembrowski WJ, Aldinger CE, Dee MF, et al. Novel, potent aldose reductase inhibitors: 3,4-dihydro-4-oxo-3-[[5-(trifluoromethyl)-2-benzothiazolyl]methyl]-1-phthalazineacetic acid (zopolrestat) and congeners. J Med Chem 1991;34:108–22.
[39] The structural assignment was based on the analysis of the ^1H and ^{13}C NMR spectra. The product 7a was further identified by determining its X-ray structure. CCDC No. 907181 (7a) contains the supplementary crystallographic data for this paper.

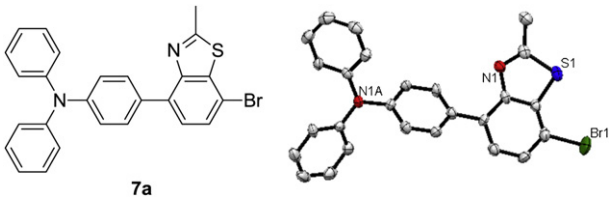

7a

[40] Guo W, Shen YH, Wu LQ, Gao YR, Ma TL. Effect of N dopant amount on the performance of dye-sensitized solar cells based on N-doped TiO_2 electrodes. J Phys Chem C 2011;115:21494–9.
[41] Suzuki A. Recent advances in the cross-coupling reactions of organoboron derivatives with organic electrophiles, 1995–1998. J Org Chem 1999;576: 147–68.
[42] Jones G. The Knoevenagel condensation. Org React 1967;15:204–599.
[43] Hao Y, Yang XC, Cong JY, Tian HN, Hagfeldt A, Sun LC. Efficient near infrared D–π–A sensitizers with lateral anchoring group for dye-sensitized solar cells. Chem Commun 2009:4031–3.
[44] Hagfeldt A, Grätzel M. Light-induced redox reactions in nanocrystalline systems. Chem Rev 1995;95:49–68.